

# Notes

## EXAFS Determinations of Uranium Structures: The Uranyl Ion Complexed with Tartaric, Citric, and Malic Acids

P. G. Allen,<sup>\*,†,‡</sup> D. K. Shuh,<sup>†</sup> J. J. Bucher,<sup>†</sup>  
N. M. Edelstein,<sup>†</sup> T. Reich,<sup>§</sup> M. A. Denecke,<sup>§</sup> and  
H. Nitsche<sup>§</sup>

Chemical Sciences Division, Lawrence Berkeley National Laboratory, Berkeley, California 94720, G. T. Seaborg Institute for Transactinium Science, Lawrence Livermore National Laboratory, Livermore, California 94551, and Forschungszentrum Rossendorf e. V., Institut für Radiochemie, Postfach 51 01 19, D-01314 Dresden, Germany

Received July 7, 1995<sup>⊗</sup>

### Introduction

Studies of the coordination chemistry of uranium in aqueous solutions are increasingly important for understanding the behavior of uranium in the environment.<sup>1–7</sup> Actinide speciation information is essential for assessing and developing long-term strategies addressing problems such as migration in nuclear waste repositories or improvements in the processing of nuclear waste and materials. Relative to the latter, one method for removing uranium contamination from soils involves extraction using a chelating agent such as Tiron, or citrate.<sup>8</sup> These types of extractants are quite efficient at binding the uranyl ion and thus are suitable for removing uranium contamination when it is in the hexavalent uranyl ion form. Martell *et al.*<sup>9,10</sup> and Markovits *et al.*<sup>11</sup> have published a series of articles detailing the complexation of the uranyl ion with tartaric, malic, and citric acids as a function of pH. Using the functional dependencies of potentiometric titration results, they showed that, in the pH range 2–4, the uranyl ion forms a 2:2 dimeric species,  $(\text{UO}_2)_2(\text{L})_2$ , where L = tartrate, malate, or citrate ligands. In considering the possible 2:2 structures shown in Figure 1, both of which involve the  $\alpha$ -hydroxyl group of the ligands for

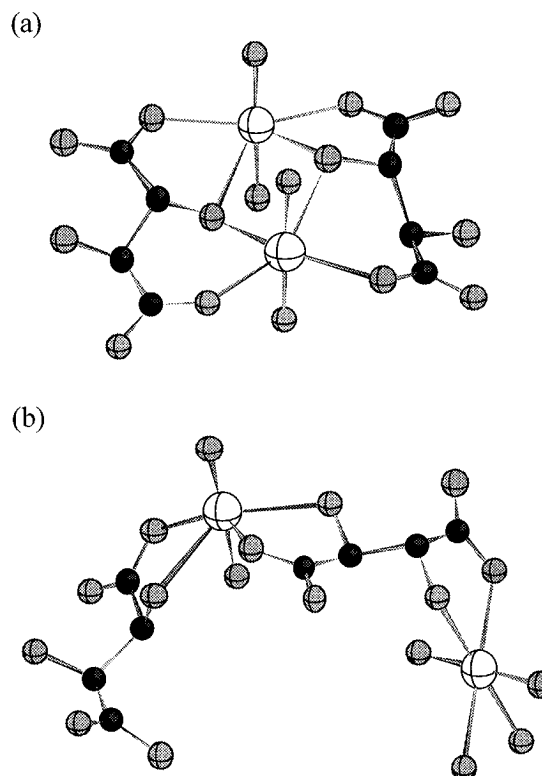


**Figure 1.** Possible structural models for the uranyl tartrate dimer having the empirical formula  $(\text{UO}_2)_2(\text{L})_2$  where L = tartrate: (a) uranyl groups are bridged by  $\alpha$ -hydroxyl groups; (b) no bridging occurs through the  $\alpha$ -hydroxyl groups.

bridging of the uranyl ions, Martell *et al.* stated a preference for the structure in Figure 1b.<sup>10</sup> However, as Martell *et al.* state, it is not possible from the titration data alone to directly distinguish between the structures shown in Figure 1 as well as other plausible 2:2 structures.

We have reinvestigated the solution structures of the uranyl complexes formed in these systems with the structural technique extended X-ray absorption fine-structure (EXAFS) spectroscopy.<sup>12</sup> Using the local structure information derived from the EXAFS spectra of these complexes in solution (i.e., bond lengths and near-neighbor types), it is possible to directly determine the dimeric structure that was inferred from earlier potentiometric titrations. Additionally, the results are applicable to models for U complexation with organic acids present in the environment such as humic acids.

### Experimental Section

**Solution and EXAFS Sample Preparation.** Materials used were reagent grade. Double-distilled deionized water was used in all preparations. A 0.08 M stock solution of the  $\text{UO}_2^{2+}$  ion was prepared by mixing uranyl nitrate,  $\text{UO}_2(\text{NO}_3)_2 \cdot 6\text{H}_2\text{O}$  (B & A, Allied Chemical & Dye Corp.), in a solution of 0.1 M nitric acid. Separate 1:1 mixtures of the uranyl ion with each ligand were prepared by mixing 10 mL of the uranyl nitrate stock solution with 10 mL of 0.2 M stock solutions of the dibasic salts  $\text{K}_2(\text{tartrate}) \cdot 0.5\text{H}_2\text{O}$  (Merck) and  $\text{Na}_2(\text{malate}) \cdot \text{H}_2\text{O}$  (Aldrich) and the tribasic salt  $\text{Na}_3(\text{citrate}) \cdot 2\text{H}_2\text{O}$  (Mallinckrodt) and diluting to 25 mL. The final pH readings of the uranyl tartrate, malate, and citrate solutions were 2.2, 2.0, and 3.8, respectively. Aliquots of 3 mL of each mixture were placed inside flexible polyethylene bags.

<sup>†</sup> Lawrence Berkeley National Laboratory.

<sup>‡</sup> Lawrence Livermore National Laboratory.

<sup>§</sup> Institut für Radiochemie.

- (1) Clark, D. L.; Hobart, D. E.; Neu, M. P. *Chem. Rev.* **1995**, *95*, 25–48.
- (2) Couston, L.; Pouyat, D.; Moulin, C.; Decambox, P. *Appl. Spectrosc.* **1995**, *49*, 349–353.
- (3) Bollinger, J. E.; Roundhill, D. M. *Inorg. Chem.* **1994**, *33*, 6421–6424.
- (4) Sayed, S. A.; Kandil, A. T.; Choppin, G. R. *J. Radioanal. Nucl. Chem.* **1994**, *188*, 377–390.
- (5) Czerwinski, K. R.; Buckau, G.; Scherbaum, F.; Kim, J. I. *Radiochim. Acta* **1994**, *65*, 111–119.
- (6) Faulques, E.; Russo, R. E.; Perry, D. L. *Spectrochim. Acta, Part A* **1994**, *50*, 757–763.
- (7) Meinrath, G.; Kato, Y.; Yoshida, Z. *J. Radioanal. Nucl. Chem.* **1993**, *174*, 299–314.
- (8) (a) Allen, P. G.; Berg, J. M.; Chisolm-Brause, C. J.; Conradson, S. D.; Donohoe, R. J.; Morris, D. E.; Musgrave, J. A.; Tait, C. D. *Symposium on Waste Management*; Arizona Board of Regents: Tucson, AZ, 1994. (b) Allen, P. G.; Berg, J. M.; Chisolm-Brause, C. J.; Conradson, S. D.; Donohoe, R. J.; Morris, D. E.; Musgrave, J. A.; Tait, C. D. Report LA-12799-PR; Los Alamos National Laboratory: Los Alamos, NM, July 1994.
- (9) Rajan, K. S.; Martell, A. E. *J. Inorg. Nucl. Chem.* **1964**, *26*, 1927–1944.
- (10) Rajan, K. S.; Martell, A. E. *Inorg. Chem.* **1965**, *4*, 462–469.
- (11) Markovits, G.; Klotz, P.; Newman, L. *Inorg. Chem.* **1972**, *11*, 2405.

Polyethylene frames (with a  $5 \times 20$  mm open slot for X-ray transmission) were placed in the bags to give rigidity to the assembly and to provide an appropriate path length for the EXAFS measurements. The resultant  $\sim 5$  mm path length and the final 0.08 M uranyl ion concentration yielded an edge jump  $\sim 0.5$  across the uranium  $L_{III}$  absorption edge. The primary polyethylene containers were heat-sealed and surrounded by a second, heat-sealed bag for safety purposes.

**EXAFS Data Acquisition and Analysis.** Uranium  $L_{III}$ -edge X-ray absorption spectra were collected at the Stanford Synchrotron Radiation Laboratory (SSRL) on wiggler beamline 4-3 (unfocused) under dedicated ring conditions (3.0 GeV, 50–100 mA) using a Si(220) double-crystal monochromator. Rejection of higher order harmonic content of the beam was achieved by detuning  $\theta$ , the angle between crystals in the monochromator, so that the incident flux was reduced to 50% of its maximum ( $>95\%$  harmonic is rejected). All spectra were collected in the transmission geometry using Ar-filled ionization chambers and a vertical slit of 0.5 mm. Three EXAFS scans were collected from each solution at ambient temperature, and the results were averaged. The spectra were energy-calibrated by simultaneously measuring the spectrum from a reference solution of 0.2 M  $UO_2Cl_2$ , which was placed between the second and third ionization chambers. The first inflection point of the absorption edge for the reference was defined as 17166 eV. EXAFS data reduction was performed by standard methods described elsewhere,<sup>12</sup> using the suite of programs EXAFSPAK developed by G. George of SSRL. Data reduction included pre-edge background subtraction followed by spline fitting and normalization (based on the Victoreen falloff) to extract the EXAFS data above the threshold energy,  $E_0$ , defined as 17185 eV. Curve-fitting analyses were performed using EXAFSPAK to fit the raw  $k^3$ -weighted EXAFS data.

The theoretical EXAFS modeling code FEFF6 of Rehr *et al.*<sup>13</sup> was employed to calculate the backscattering phases and amplitudes of the individual neighboring atoms for the purpose of curve-fitting the raw data. All of the interactions modeled in the fits were derived from FEFF6 single- or multiple-scattering (SS or MS) paths calculated for the model compound  $UO_2(CH_3COO)_2 \cdot 2H_2O$ .<sup>14</sup> The relevant paths that FEFF6 calculates for this model compound are SS U–O (axial), SS U–O (equatorial), SS U–C (from the bidentate acetate ligand), SS U–U, MS O–U–O (4-legged path), and MS U–C–C (3- and 4-legged paths). The amplitude reduction factor,  $S_0^2$ , was held fixed at 0.9 for all of the fits. The shift in threshold energy,  $\Delta E_0$ , was allowed to vary as a global parameter in each of the fits (i.e., the same  $\Delta E_0$  was used for each shell).

## Results and Discussion

Figure 2 shows the raw  $k^3$ -weighted EXAFS data for the uranyl tartrate, malate, and citrate solutions. Solely on the basis of the raw data, the U polycarboxylate spectra show a strong similarity. There is close agreement among the three samples in the phase as well as in the amplitude of all the features in  $k$  space. Similarly, the  $R$ -space plots of the Fourier-transformed EXAFS data shown in Figure 3 are also in close agreement. The Fourier transforms (FTs) represent a pseudoradial distribution function of the uranium near-neighbor environment, and the peaks appear at lower  $R$  values relative to the true near-neighbor distances as a result of the EXAFS phase shifts which are different for each neighboring atom ( $\alpha = 0.2$ – $0.5$  Å). The FTs illustrate that the EXAFS is dominated by scattering from the O atoms of the linear  $UO_2^{2+}$  group (peak at 1.30 Å) and scattering from the O atoms lying in the equatorial plane of the  $UO_2^{2+}$  ion (peak at 1.90 Å). In addition, the FTs show the presence of another interaction at *ca.* 3.75 Å which is reproduced in each solution. The portion of the FT above 4 Å can be used

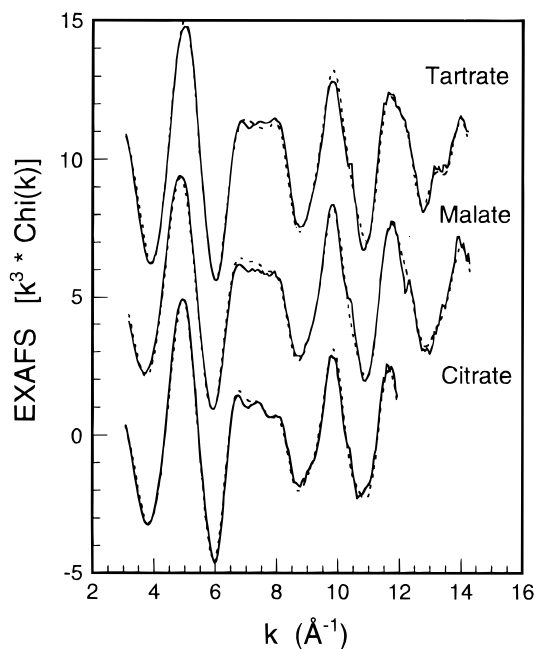


**Figure 2.** Raw  $U L_{III}$ -edge  $k^3$ -weighted EXAFS data for 1:1 mixtures of uranyl with tartrate, malate, and citrate ligands at low pH. The solid lines are the experimental data, and the dashed lines are the best theoretical fits of the data.

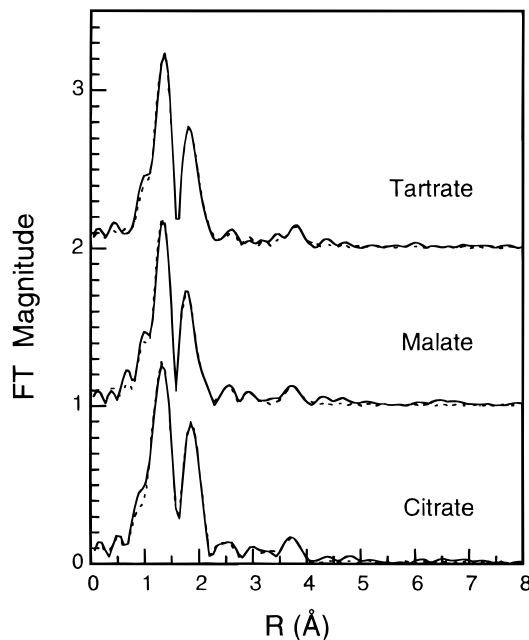


**Figure 3.** Fourier transforms of  $U L_{III}$  EXAFS data for 1:1 mixtures of uranyl with tartrate, malate, and citrate ligands at low pH. Transforms were taken over the range of the data shown in Figure 2. The solid lines are the experimental data, and the dashed lines correspond to the best theoretical fits of the data. The U–U peak at 3.75 Å (uncorrected for phase shift) is evidence for the dimeric structure in Figure 1a.

to gauge the noise level in the EXAFS signal. Considering the fact that the FT above 4 Å is featureless and smooth, the 3.75 Å peak is the result of a real interaction, rather than an experimental artifact.

Modeling and curve-fitting analyses were performed on the raw EXAFS data to determine the bond lengths and coordination numbers and to examine the origin of the peak at 3.75 Å. The data ranges used in the fitting procedure were 3–14 Å<sup>-1</sup> for the tartrate and malate solutions and 3–12 Å<sup>-1</sup> for the citrate solution. The structural results are summarized in Table 1. Each sample shows  $\sim 2$  O at 1.78 Å, indicative of axial oxygen atoms

(12) Prins, R.; Koningsberger, D. E. *X-ray Absorption: Principles, Applications, Techniques for EXAFS, SEXAFS, and XANES*; Wiley-Interscience: New York, 1988.

(13) Rehr, J. J.; Mustre de Leon, Zabinsky, S.; Albers, R. C. *Phys. Rev. B* **1991**, *44*, 4146.

(14) Howatson, J.; Grev, D. M.; Morosin, B. *J. Inorg. Nucl. Chem.* **1975**, *37*, 1933–1935.

**Table 1.** EXAFS Structural Results for  $(\text{UO}_2)_2(\text{L})_2$  Complexes

	$R$ (Å) <sup>a</sup>	$N$	$\sigma^2$ (Å <sup>2</sup> ) <sup>b</sup>	$\Delta E_0$ (eV)	$F$
$(\text{UO}_2)_2(\text{tartrate})_2$					
U–O <sub>ax</sub>	1.78	2.3	0.0027	–9.8	0.0543
U–O <sub>eq1</sub>	2.35	3.1	0.0035		
U–O <sub>eq2</sub>	2.47	2.3	0.0045		
U–C	2.92	2.0	0.0069		
U–U	3.95	0.5	0.0020		
$(\text{UO}_2)_2(\text{malate})_2$					
U–O <sub>ax</sub>	1.78	2.3	0.0022	–9.6	0.0625
U–O <sub>eq1</sub>	2.33	2.7	0.0034		
U–O <sub>eq2</sub>	2.45	2.7	0.0045		
U–C	2.94	2.0	0.0047		
U–U	3.93	0.7	0.0045		
$(\text{UO}_2)_2(\text{citrate})_2$					
U–O <sub>ax</sub>	1.78	2.3	0.0035	–3.3	0.0331
U–O <sub>eq1</sub>	2.38	5.0	0.0068		
U–C	2.94	2.0	0.0056		
U–U	3.93	1.3	0.0070		

<sup>a</sup> Errors in distances ( $\pm 0.02$  Å) and coordination numbers ( $\pm 20\%$ ) are estimated from the deviation between fitting results from models of known structures and their true values. <sup>b</sup>  $\sigma$  = Debye–Waller factor.

on the uranyl group. A relatively weak multiple-scattering interaction at  $3.56$  Å originating from the 4-legged path along the O–U–O vector (twice the U–O<sub>ax</sub> distance) was also included in the fits. Rather than being varied independently, this path was linked directly to floating bond lengths ( $R$ ) and coordination number ( $N$ ) values of the axial oxygen shell.<sup>15</sup> The equatorial plane around the uranyl group contains  $\sim 5$  O at *ca.*  $2.40$  Å in each of the samples. The tartrate and malate data sets extended out to higher  $k$  values, which permitted the resolution of the equatorial O shell into two components with different U–O distances.<sup>16</sup> Using 2 shells rather than 1 shell of equatorial oxygen atoms, the normalized  $F$  values of the fits improved from 0.090 to 0.053 and from 0.084 to 0.062 for the tartrate and malate fits, respectively.<sup>17</sup> The fits also show 2 C atoms at *ca.*  $2.9$  Å. The presence of C neighbors in the EXAFS confirms ligation directly to the tartrate, malate, and citrate ligands at the carboxylate or the  $\alpha$ -hydroxyl groups. The observation of two different equatorial O shells may be explained by the presence of different U–O bond lengths for oxygens in the carboxylate groups, the  $\alpha$ -hydroxyl groups, and water molecules—each of which may be present in the equatorial plane of the uranyl group. For example, in the structures of vanadium and antimony tartrate complexes the metal–oxygen bond lengths for the carboxylate oxygen atoms are longer than those for the hydroxyl oxygen atoms.<sup>18,19</sup> With respect to our fitting results, a plausible model would be the one shown in Figure 1a. In this model, each uranium atom would see 2 carboxylate oxygens at  $R_1$  and 2 hydroxyl oxygens at  $R_2$ , where  $R_1 > R_2$ . Filling the equatorial coordination sphere to the value obtained in our fits,  $N_O \sim 5$ , would require  $\sim 1$  water molecule.

(15) Allen, P. G.; Bucher, J. J.; Clark, D. L.; Edelstein, N. M.; Ekberg, S. A.; Gohdes, J. W.; Hudson, E. A.; Kaltsoyannis, N.; Lukens, W. W.; Neu, M. P.; Palmer, P. D.; Reich, T.; Shuh, D. K.; Tait, C. D.; Zwick, B. D. *Inorg. Chem.* **1995**, *34*, 4797.

(16) For shells of identical backscatterers occurring at two different distances  $R_1$  and  $R_2$ , an interference beat will occur in the EXAFS at  $k = \pi/2(R_1 - R_2)$ . The results in Table 1 indicate that a beat occurs at  $k \sim 13$  Å<sup>-1</sup>. Since our data extend to  $k = 14$  Å<sup>-1</sup>, it is possible to resolve two distances separated by  $0.12$  Å (see ref 12).

(17)  $F$  is a goodness of fit parameter defined as  $F = \sum k^6(\text{data} - \text{fit})^2 / (N_{\text{pts}} - N_{\text{var}})$  where  $N_{\text{pts}}$  is the number of data points and  $N_{\text{var}}$  is the number of floating variables.

(18) Pizarro, J. L.; Garcia-Jaca, J.; Rojo, T.; Arriortua, M. I. *Acta Crystallogr. Sect. C: Cryst. Struct. Commun.* **1994**, *50*, 1394–1396.

(19) Gress, M. E.; Jacobson, R. A. *Inorg. Chim. Acta* **1974**, *8*, 209.

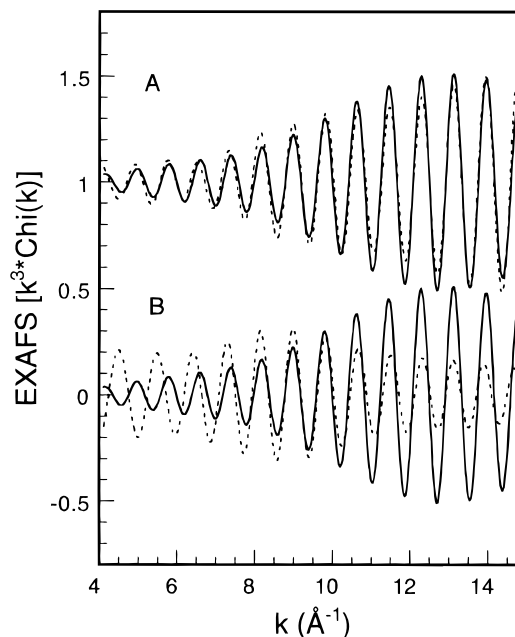


**Figure 4.** Fits to the Fourier-filtered peak at  $3.75$  Å using (A) one SS U–U path and (B) a sum of 3-legged and 4-legged MS U–C–C paths as described in the text. The solid lines are the experimental data, and the dashed lines correspond to the best fits.

However, the corresponding U–O<sub>water</sub> bond length is likely to be unresolvable from either of the other two shells.

In an investigation of the nature of the  $3.75$  Å peak, this contribution was isolated by taking the difference between the uranyl tartrate data and a fit which included only the near-neighbor contributions mentioned above.<sup>20</sup> The residual obtained by this procedure contains only those contributions unaccounted for in the fit—specifically the interaction appearing at  $3.75$  Å. The residual EXAFS signal was Fourier-filtered over the range  $3.2$ – $4.2$  Å to remove noise in the fit,<sup>12</sup> and is shown in Figure 4. Even at this level of analysis, the increasing EXAFS amplitude as a function of  $k$  is a signature of backscattering from an atom of relatively high  $Z$ . The corresponding single U shell fit (Figure 4a) confirms this assignment. The only other possible source of this peak would be scattering along paths involving the low- $Z$  ligands C or O centers. Low- $Z$  atoms are not normally detected in room-temperature solutions at  $R > 3$  Å, unless a MS enhancement of the amplitude is operative. Examples for uranium systems have been observed when ligands like carbonate or nitrate adopt a symmetric bidentate geometry where the distal O atom is collinear with the absorbing atom and the C or N atoms.<sup>15,21</sup> Thus, the most plausible alternative explanation for the peak at  $3.75$  Å is bidentate ligation of the carboxylate groups (i.e., a U–C<sub>1</sub>–C<sub>2</sub> path). However, the phase and amplitude derived from a sum of 3-legged (U → C<sub>1</sub> → C<sub>2</sub> → U) and 4-legged (U → C<sub>1</sub> → C<sub>2</sub> → C<sub>1</sub> → U) MS paths offer a poor match to the data (Figure 4b). In addition, the resulting U–C<sub>2</sub> bond length of  $4.24$  Å would give the C<sub>1</sub>–C<sub>2</sub> bond length at  $1.31$  Å which is inconsistent with the C–C bond length of  $1.53$  Å determined for  $\text{UO}_2(\text{CH}_3\text{COO})_2 \cdot 2\text{H}_2\text{O}$ .<sup>14</sup>

The fitting results obtained by the inclusion of a U–U interaction along with the O and C shell contributions described above are summarized in Table 1. The fits to the EXAFS data

(20) Allen, P. G.; Mustre de Leon, J.; Conradson, S. D.; Bishop, A. R. *Phys. Rev. B* **1991**, *44*, 9480.

(21) Veirs, D. K.; Smith, C. A.; Berg, J. M.; Zwick, B. D.; Marsh, S. F.; Allen, P. G.; Conradson, S. D. *J. Alloys Compd* **1994**, *213/214*, 328–332.

and FTs of each are shown in Figures 2 and 3, respectively. Combining the results with those of Martell *et al.*,<sup>9,10</sup> it is now possible to more definitively assign a structure to the 2:2 dimer present in these solutions. The structure in Figure 1b is ruled out on the basis that a U–U interaction at 3.9 Å, if configurationally allowed, would not be detected due to dynamic disorder in the solution. Another relevant dimeric structure that can be discounted has been observed by X-ray diffraction in solid vanadium and antimony compounds that contain a distinct  $M_2(\text{tartrate})_2$  unit.<sup>18,19</sup> In these examples, the V–V and Sb–Sb distances are 4.24 and 5.08 Å, respectively. Thus, in an identical arrangement of the tartrate ligands with the uranyl groups, a U–U distance of 3.95 Å, which is substantially shorter than the analogous V–V and Sb–Sb distances, would not be possible.<sup>22</sup>

Apart from the structure shown in Figure 1a, the only other structure that could possess a U–U interaction at 3.95 Å would be a hydrolysis product,  $(\text{UO}_2)_2(\text{OH})_2^{2+}$ .<sup>23,24</sup> However, equilibrium calculations using the computer code HYDRAQL<sup>25</sup> and considering the numerous equilibria involved show that the

concentrations of  $(\text{UO}_2)_2(\text{OH})_2^{2+}$  and other hydrolysis products are several orders of magnitude smaller than the concentration of  $(\text{UO}_2)_2(\text{L})_2$ . In contrast, the calculations indicate that the amount of the free uranyl aquo ion,  $\text{UO}_2^{2+}$ , is significant at low pH. For the uranyl tartrate and malate solutions at pH ~ 2, the molar ratio of  $\text{UO}_2^{2+}$  to  $(\text{UO}_2)_2(\text{L})_2$  is 2:1. For the uranyl citrate solution at pH = 3.8, the ratio is 1:20. Since EXAFS is an atomic property and is averaged over the total U present in each species, the calculated value for the U coordination number,  $N_U$ , would be 0.5 at pH = 2 and 1.0 at pH = 3.8. This result is supported by the curve-fitting results in Table 1 which give  $N_U = 0.5$  and 1.3 for the tartrate and citrate solutions, respectively. Although the Debye–Waller factors are correlated in the fitting results ( $\sigma$  gets larger with  $N$ ), the integrated amplitudes<sup>26</sup> of the U–U contributions from the tartrate and citrate solutions remain in a constant 1:2 ratio. Thus, the equilibrium calculations further rule out certain structures and confirm the type of structure depicted in Figure 1a for the formation of these  $(\text{UO}_2)_2(\text{L})_2$  dimers.

**Acknowledgment.** This work was supported by the Director, Office of Energy Research, Office of Basic Energy Sciences, Chemical Sciences Division, U.S. Department of Energy, under Contract No. DE-AC03-76SF00098. This work was done (partially) at SSRL, which is operated by the Department of Energy, Division of Chemical Sciences.

IC9508536

- 
- (22) In this arrangement, the tartrates are quadridentate and bridging. There is bidentate coordination to a metal atom at each end of the tartrate using a single oxygen atom from each of the hydroxyl and carboxylate groups. For the uranyl group to adopt this geometry, the two linear  $\text{UO}_2^{2+}$  groups would have to align end-to-end, which seems implausible. Additionally, the same quadridentate ligation is not possible for the malate or citrate ligands.
- (23) Ahrland, S. In *Handbook on the Physics and Chemistry of the Actinides*; Freeman, A. J., Keller, C., Eds.; Elsevier Science Publishers: Amsterdam, 1991.
- (24) Mixed-ligation species, such as a dimer with one hydroxide and one alkoxide bridge, are ruled out from the potentiometric titration results which find a 2:2 ratio of uranyl ion to tartrate, malate, or citrate ligands.

- 
- (25) Papelis, C.; Hayes, K. F.; Leckie, J. O. HYDRAQL: A Program for the Computation of Aqueous Batch Systems Including Surface Complexation Modeling of Ion Adsorption at the Oxide/Solution Interface. Technical Report 306; Department of Civil Engineering, Stanford University: Stanford, CA, 1988.
- (26) The integrated amplitude is calculated from the integral  $\int N \exp(-\sigma^2 k^2)$  taken over a given  $k$  range and is used as a measure of the relative magnitudes of the EXAFS components.